Tellus
SERIES A DYNAMIC METEOROLOGY AND OCEANOGRAPHY
PUBLISHED BY THE INTERNATIONAL METEOROLOGICAL INSTITUTE IN STOCKHOLM

Tellus (2008), 60A, 649–662
Printed in Singapore. All rights reserved

TELLUS

A statistical approach for sedimentation inside a microphysical precipitation scheme

By J.-F. GELEYN[1]*, B. CATRY[2], Y. BOUTELOUP[3] and R. BROŽKOVÁ[1], [1]*ONPP, Czech Hydrometeorological Institute, Prague-Komořany, Czech Republic;* [2]*Sterrenkundig Observatorium, Ghent University, Ghent, Belgium;* [3]*Centre National de Recherches Météorologiques, Météo-France, Toulouse, France*

(Manuscript received 16 July 2007; in final form 4 February 2008)

ABSTRACT

A statistical approach for the sedimentation of prognostic precipitating species inside a microphysical scheme is proposed. The unique fall speed of precipitation used by a typical advective scheme is replaced by three probabilities of transfer associated with the following three types of precipitation: (i) precipitation present in the layer at the beginning of the time step; (ii) precipitation coming from the layer above which crosses the layer under consideration and (iii) precipitation locally produced (or destroyed) during the time step. The use of a decreasing exponential Probability Distribution Function (PDF) as basis for these probabilities ensures that the normalized probabilities do not depend on the origin of the precipitation. The main advantage of this characteristic is that the sedimentation process can now be computed in a single vertical loop. Other functions can also be used as basis for the probabilities and the case with a step function is discussed. The performance of the proposed PDF-based sedimentation scheme is validated in an academic single column model and in a full 3-D framework.

1. Introduction

A never-ending increase in computer power allows many Numerical Weather Prediction (NWP) communities to develop more realistic and consequently more complex schemes that describe physical processes occurring in the earth-atmosphere system. A microphysical scheme that describes the complete evolution of moisture in all its forms and phases is perhaps one of the most complex ones.

Not so long ago only water vapour, liquid suspended water and solid suspended water were treated as prognostic quantities inside a microphysical scheme, whereas rain and snow were computed diagnostically from their respective budget quantities. The recent arrival of new schemes at an intermediate complexity level (e.g. Schultz 1995; Reisner et al., 1998; Wilson and Ballard, 1999; Lopez, 2002; Dare, 2004; Seifert and Beheng, 2006, to name only a few) marked an increase of the number of prognostic water species in the direction of falling precipitations. Many NWP-type models nowadays treat (even in operational setups) the five traditional water species (water vapour, suspended liquid water, suspended ice, rain-water and snow) in a prognostic way and in the future this will most likely be extended with the arrival of other ice-phase species like graupel and hail.

Apart from the thermodynamic consequences related to such an extended set of prognostic variables (see e.g. Catry et al., 2007), the upgrade of rain and snow to prognostic variables also requires a sound physical and numerical description of the evolution of these species. One of the main aspects in this evolution is the interaction of the falling species (rain and snow) with the environment along their trajectory. Processes such as collection, evaporation of precipitation, their melting-freezing, etc. will have a significant impact on the final rain and snow fluxes leaving a model layer. The vertical sedimentation of falling species should therefore be treated very carefully. In most (if not all) microphysical schemes sedimentation is treated by an advective transport scheme which uses a unique (mean) fall speed for each kind of precipitation, even though suppressing the dispersive properties of falling precipitations surely puts one away from reality. Indeed, the variety in raindrop sizes (resulting from many processes like collection, growth, evaporation, splitting, etc.) and the equilibrium between gravity and friction results in a variety of observed fall speeds in nature.

Inside the Action de Recherche Petite Echelle Grande Echelle/Aire Limitée Adaptation dynamique Développement International (ARPEGE/ALADIN) community, the upgrade of rain and snow to prognostic species created an opportunity to revisit the problem of sedimentation of precipitation inside the microphysical scheme. The previous diagnostic type microphysical scheme however did have one big advantage: it used a single vertical loop for computing all processes acting on the

*Corresponding author:
e-mail: Jean-Francois.Geleyn@chmi.cz
DOI: 10.1111/j.1600-0870.2008.00323.x

precipitation fluxes. When upgrading the scheme to a prognostic version, it was sought to preserve this cost-efficient single vertical loop construction if feasible. Clearly, a typical advective scheme of the Lagrangian type (which requires a double vertical loop) immediately falls out of this scope. On the other hand, an advective scheme of the Eulerian type (which uses a single loop) needs a lot of iterations within the time step in order to cope with the vertical Courant–Friedrichs–Lewy (CFL) limitation, which makes this method quite expensive by forcing the time step to be sufficiently short so that its product by the advection speed does not exceed the layer's thickness anywhere along the vertical.

In this paper, we will propose a statistical approach for sedimentation of precipitation and we will show that this approach is more flexible than a pure advective scheme. What is more, we shall demonstrate that the statistical approach can also mimic an advective sedimentation scheme under some specific constraints. The physical basis of the method is presented in Section 2, whereas its mathematical counterpart is developed in detail in Section 3. The performance of the scheme is validated in Sections 4 and 5 by using, respectively, an academic single column model and the full 3-D so-called ALARO-0 framework. Finally, some conclusions are drawn in Section 6.

2. The statistical approach

The upgrade of a pure diagnostic microphysical scheme towards a prognostic one starts evidently with the introduction of prognostic precipitating species. This paper shall be restricted to the introduction of rain. The extension for other precipitating species such as snow, graupel and/or hail, is completely similar and is left to the reader. The quantity of rain will be represented by its mass ratio q_r with respect to the total mass of the parcel of air.

When trying to find an alternative for the unique fall speed in an advective sedimentation scheme, it seems only natural to look for a more statistical treatment of the fall speed. This can be achieved by replacing the single fall speed by a spectrum of fall speeds going from zero to infinity, while the above mentioned unique fall speed is the mass-weighted average of this spectrum, that is, the first moment of the associated Probability Density Function (PDF). For a given time interval (typically the model's time step) the PDF of velocities can easily be converted in one of 'reachable distances along the vertical' which falling species can travel during this time interval. With an infinity of trajectories to handle one seems to be in an even worse situation than previously (regarding the interaction between sedimentation and other microphysical processes). But let us assume that this PDF is forced to always be a decreasing exponential $P_0 = \exp[-\delta z/(\overline{w}\delta t)]$, with δz the crossed distance, $\overline{w}$ the mean fall speed and δt the time interval. Then one can use the fundamental property (similar to the one of constant life expectancy of a radioactive isotope during its disintegration) that the normalized probabilities are identical whatever the origin of the drops leaving a model layer through its bottom.

In the sedimentation scheme which will be presented below, three 'sources' of precipitation with each an associated special probability of contributing to the precipitation flux at the bottom of the layer will be taken into account: (i) precipitation already present in the layer at the beginning of the time step (probability P_1); (ii) precipitation coming from the layer above (probability P_2) and (iii) precipitation locally produced (or destroyed) by processes such as autoconversion, collection and evaporation plus melting-freezing (probability P_3).

One can combine the weighted probabilities of these three sources to get a unique flux-type output at the bottom of the layer and thus at the top of the next one below, this allowing to repeat the same computations everywhere within a single vertical loop. Indeed, in the layer below, one will not need any information on the origin of the precipitation which comes through the top of that layer. The precipitation travelling across the layer can of course still undergo local processes such as phase changes, accretion, coalescence, etc. In short, the cumbersome advective treatment of sedimentation has been replaced by an elementary statistical one.

Note that if one assumes an infinite average fall speed, the method above immediately degenerates in the one used in the previous diagnostic version of the microphysical scheme where the precipitation was removed in one time step (see Geleyn et al., 1994). This helps explaining why this choice, apart from other advantages, was for us the best one for the upgrade towards a prognostic version of the scheme.

Since there is now little risk to get advection-related numerical problems with such an enhancement, one may also introduce an observed-like dependency of the average fall speed upon the intensity of the precipitation flux. Strictly speaking this is not compatible with the additivity rule central to the proposal, but since one shall have to deal with rather small variations of the parameter across each model layer, it is numerically acceptable (and more realistic of course).

3. The probabilities

3.1. Expressions using a decreasing exponential

As mentioned above, one assumes that the PDF P_0 is a function of the average fall speed $\overline{w}$, of the model layer thickness δz and of the time step δt. Defining $P_0(z, t) = \exp[-z/(\overline{w}t)]$ one can compute the three above-mentioned probabilities of 'escape' as described below.

(1) *First case:* Raindrops present inside the layer at the beginning of the time step. It is realistic to assume that the drops are homogeneously distributed in space. Hence

$$P_1(\delta z, \delta t) = \frac{1}{\delta z}\int_0^{\delta z} P_0(z, \delta t)\,\mathrm{d}z = \frac{\overline{w}\delta t}{\delta z}\left(1 - \mathrm{e}^{-\dfrac{\delta z}{\overline{w}\delta t}}\right).$$

Introducing $Z = \delta z/(\overline{w}\delta t)$ (i.e. the inverse of the Courant number) one can write

$$P_1(Z) = \frac{1 - P_0(Z)}{Z}. \tag{1}$$

(2) *Second case:* Raindrops coming from the layer above. A homogeneous arrival in time (of the drops) at the top is a reasonable assumption, hence

$$P_2'(\delta z, \delta t) = \frac{1}{\delta t}\int_0^{\delta t} P_0(\delta z, t)\,\mathrm{d}t = \frac{1}{\delta t}\int_0^{\delta t} \mathrm{e}^{-\dfrac{\delta z}{\overline{w}t}}\,\mathrm{d}t = E_2(Z),$$

with $E_2(Z)$ the second exponential integral which can be approximated such that

$$P_2'(Z) = E_2(Z) \approx \frac{P_0(Z)}{Z + 1 + X} \tag{2}$$

with

$$X = \frac{\sqrt{(1+Z)^2 + 4Z} - (1+Z)}{2}.$$

The link between P_2' and the final P_2 will be explained below, after the derivation of the related P_3 function.

(3) *Third case:* During the time step raindrops are created (or destroyed) inside the layer. One can now assume a homogeneous production in both space and time resulting in the convolution of the two previous integrals:

$$\begin{aligned} P_3(\delta z, \delta t) &= \frac{1}{\delta z \delta t}\int_0^{\delta z}\int_0^{\delta t} P_0(z, t)\,\mathrm{d}t\,\mathrm{d}z \\ &= \frac{1}{\delta z}\int_0^{\delta z} E_2\left(\frac{z}{\overline{w}\delta t}\right)\mathrm{d}z = \frac{1}{Z}\left[\frac{1}{2} - E_3(Z)\right], \end{aligned}$$

with E_3 the third exponential integral. The expression above can be approximated by

$$P_3(Z) = \frac{1}{Z}\left[\frac{1}{2} - E_3(Z)\right] = \frac{1}{2}[E_2(Z) + P_1(Z)] \tag{3}$$

$$= \frac{1}{2}[P_2'(Z) + P_1(Z)], \tag{4}$$

where one used the exact recurrence relationship between E_3 and E_2 $[2E_3(Z) + ZE_2(Z) = \exp(-Z)]$.

In the remainder of the paper, a more intuitive notation will be used to represent the various probabilities, whenever this does not interact with algebraic expressions and/or figure captions. We have the following identifications:

(i) $P_1 \equiv P_{\mathrm{local}}$ (because this function acts on the falling species locally present in the layer at the beginning of the time step)

(ii) $P_2' \equiv P_{\mathrm{trans}}$ (because this function corresponds to the simplest way to compute the transmission of the precipitation flux across the layer)

(iii) $P_2 \equiv P_{\mathrm{trans\_sta}}$ (because the transmission-like function is modified to obey a stationarity constraint (cf. Section 3.2))

(iv) $P_3 \equiv P_{\mathrm{cre/des}}$ (because this function corresponds to the export (or non-export) of species created (or destroyed) within the layer during the time step).

These notations will be extended to the Q-functions defined in Section 3.3.

One has to realize here that the introduction of the time integral in the derivation of eq. (3) [alike for the derivation of eq. (2)], is meant to ensure a consistent treatment between all kinds of possible sources for the flux resulting from the continuous transfer of falling species from the considered model layer into the one below. Since the processes leading to the creation or disappearance of falling species' particles are highly complex, it will not be possible to use the idealized tools of Section 4 to study the validity of this approach. But it will be shown below that one method of comparison with Lagrangian-type sedimentation schemes can be designed (with a PDF Q_0 differing from the above P_0 one). In such a case, with quasi-equivalent sedimentation computations, the verified agreement between the precipitation amounts in a full 3-D framework (not shown) indirectly validates the way we elected to derive the $P_{\mathrm{cre/des}}$ probability function.

In fact, this method for deriving $P_{\mathrm{cre/des}}$ is equivalent to say that the separately computed processes for autoconversion or collection or evaporation of falling species (etc.) are assumed evenly distributed in space and time and that this assumption is directly reflected in the (implicit) choice of the particle trajectories that are added or suppressed within the statistical computation of sedimentation. These additions and suppression are in fact part of the mechanism maintaining the shape of the PDF P_0, but we do not need to explicit this link in the proposed mathematical framework.

Coming back to the choice of the basic P_0 PDF, it must be stressed that its aim is double: physically, one wishes to get away from the non-dispersive character of the advective sedimentation methods, which require to assume a single fall speed for all particles; mathematically, one wants to ensure that the implied shape of the three resulting practical probability functions will be the same, something that automatically leads to the decreasing exponential shape. Like in all other cases (analytical fit to observed distributions, single fall-speed) the preservation of this shape requires a 'deus ex machina' mechanism having to do with the creation and destruction processes that will ultimately be handled under the $P_{\mathrm{cre/des}}$ probability. In that sense the chosen basic mathematical constraint is a priori neither more physically realistic than those of competing choices, nor less. But the introduction of dispersive properties directly in the sedimentation computation ought to be a positive feature when it comes to fit spectrally detailed reference computations. These issues will be further addressed in Section 3.5 and in Section 4.

3.2. *Corrected expressions (for the decreasing exponential case)*

The initial academic single column tests (see Section 4) with the three functions above did not meet expectations. There are at least three reasons for these first poor results (which seemed linked with the expression of P_{trans}) and how to counter them will be demonstrated below. The search for a consistent expression for $P_{\mathrm{trans\_sta}}$ starts with the assumption that the expressions of P_0 and P_{local} are correct.

First, the above derivation of P_{trans} and $P_{\mathrm{cre/des}}$ does not take into account what kind of redistribution happens between the various terms within the layer along the time step. Processes like evaporation and melting or freezing of precipitation need to be taken into account in order to be compatible with the flux-driven balance equations which will ultimately be used to compute the evolution of falling species (see again Catry et al., 2007). One must therefore look further at the problem under a double angle: the stationary solution (q_r is constant) and the full evolution equation of q_r when no stationarity is warranted.

In the stationary case one can write

$$\frac{\partial q_r}{\partial t} \equiv 0 \Rightarrow P_l^{\mathrm{bot}} - P_l^{\mathrm{top}} = \frac{\delta p}{g\delta t}(\Delta q^{\mathrm{aco}} - \Delta q^{\mathrm{evap}}) \tag{5}$$

with P_l^{top} and P_l^{bot}, respectively, the liquid precipitation fluxes through the top and bottom of the layer, p the air pressure, g the gravitational acceleration, Δq^{aco} the increase in rain-water due to autoconversion and Δq^{evap} the loss of rain-water due to evaporation of precipitation (both being generic names and expressions for a class of processes). By definition one also has

$$P_l^{\mathrm{bot}} = q_r \frac{\delta p}{g\delta t} P_1 + P_l^{\mathrm{top}} P_2 + \frac{\delta p}{g\delta t}(\Delta q^{\mathrm{aco}} - \Delta q^{\mathrm{evap}}) P_3. \tag{6}$$

Combining both expressions yields

$$P_l^{\mathrm{bot}}(1 - P_3) = P_l^{\mathrm{top}}(P_2 - P_3) + q_r \frac{\delta p}{g\delta t} P_1. \tag{7}$$

A sound physical solution for the stationary case can only be obtained when $P_2 \geq P_3$, since otherwise an increase of the flux at the top would lead to a decrease of the flux at the bottom, all other things unchanged.

Let us now consider the case when using a full evolution equation for q_r. The P_{local} and $P_{\mathrm{cre/des}}$ parts in the derivation in the previous subsection can be seen as intangible values resulting from the computation of

$$\frac{1}{\delta z}\int_0^{\delta z}\left[P_0(z,\delta t)\, q_r + \frac{1}{\delta t}\int_0^{\delta t} P_0(z,t)(\Delta q^{\mathrm{aco}} - \Delta q^{\mathrm{eva}})\,\mathrm{d}t\right]\mathrm{d}z$$

$$= \frac{1}{\delta z}\int_0^{\delta z}\left[\frac{1}{\delta t}\int_0^{\delta t} P_0(z,t)\,\tilde{q}_r(t)\,\mathrm{d}t\right]\mathrm{d}z, \tag{8}$$

with $\tilde{q}_r(t)$ a time dependent rain-water ratio which takes the effects of evaporation of precipitation and autoconversion inside the layer into account. The true evolution equation of q_r however will also contain a term coming from the vertical divergence of the precipitation flux which is consequently related to $P_{\mathrm{trans\_sta}}$. One may start by saying that the part of the flux at the top of the layer which will not be subject to the P_{trans} 'direct' transfer will create a source term inside the layer which will then be subject to $P_{\mathrm{cre/des}}$ (after some necessary 'deus ex machina' vertical homogenization inside the layer). One can thus write

$$P_2 = P_2' + (1 - P_2')P_3. \tag{9}$$

Since the corresponding outgoing part will create a sink which will lower the part of the effect proportional to $(1 - P_2')$, this is a biased answer. The multiplier will then be, in first approximation, $P_3 - P_3^2$. But then there is again a source term so that the multiplier becomes $P_3 - P_3^2 + P_3^3$. And so on. One finally finds (with the compact expression for an infinite series)

$$P_2 = P_2' + \frac{(1 - P_2')P_3}{1 + P_3} \quad \text{or} \quad P_{\mathrm{trans\_sta}} = P_2 = \frac{P_2' + P_3}{1 + P_3}. \tag{10}$$

This expression warrants $P_2 \geq P_3$ only when $Z \leq 0.96$ (see upper panel of Fig. 1). For bigger values of Z the difference between $P_{\mathrm{trans\_sta}}$ and $P_{\mathrm{cre/des}}$ is however always very small (maximum

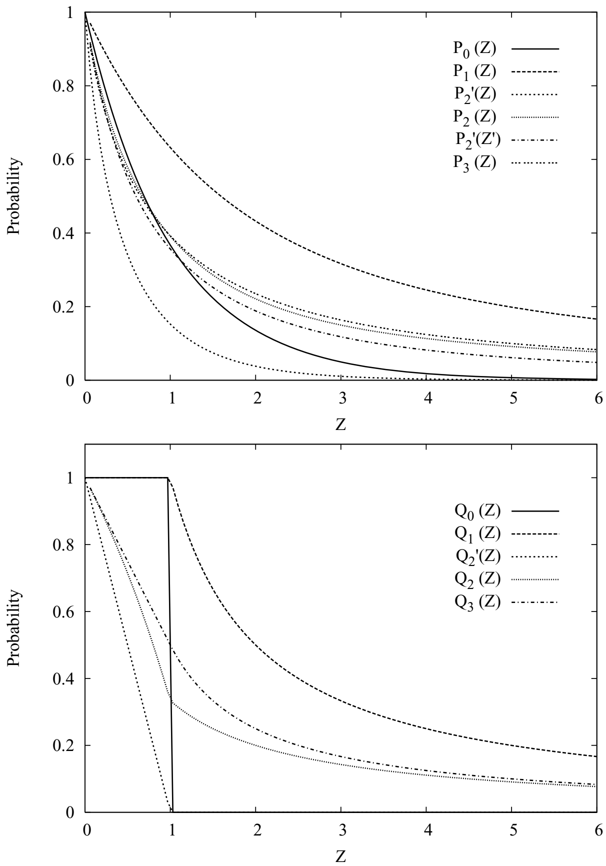

Fig. 1. Upper panel: The initial and corrected probabilities associated with the PDF P_0 (decreasing exponential) as functions of Z (inverse of the Courant number). Lower panel: The probabilities related to the PDF Q_0 (step function) as functions of the same Z.

deviation of 0.015 for $Z \sim 2.4$). Anyhow, for the stationary path to work, one needs the mean Courant number C (inverse of Z) to be big enough for making the vertical redistribution hypothesis plausible (which is required when using a budget equation for an assumed homogeneous q_r). Below a certain value ($C \sim 1.04$) this is not the case any more. This may of course be considered as an intrinsic weakness of the statistical sedimentation proposal, but any advective method will suffer from a similar drawback (the advected species may still be at the top of the layer and will have to be redistributed at the end of the time step). Here we can quantify this drawback and say for which values of Z or C it starts to be present and how small the difference between $P_{\mathrm{trans\_sta}}$ and $P_{\mathrm{cre/des}}$ anyhow remains.

Second, the derivation of the expression for P_{trans} assumes a homogeneous arrival in time of raindrops at the top of a layer. This assumption might be a bit too far from the truth. Indeed, comparison of the figures shown in Section 4, tells us that when using a spectrum of fall speeds (which is closer to observations than a single fall speed for all raindrop sizes) the accumulation of rain-water through a surface grows faster than when using a constant fall speed. So, apart from the rain-water which by definition contributes to P_{trans} there is an additional source of water which is subject to $P_{\mathrm{cre/des}}$. In fact this brings us back to the case described above, that is, the change from P_{trans} to $P_{\mathrm{trans\_sta}}$.

Finally, it appeared that the choice of Z is not so straightforward. Indeed, P_{local} is associated with precipitation which has the characteristics (i.e. Z) of the layer under consideration. On the other hand, P_{trans} is associated with precipitation coming from the layers above and is consequently characterized by a different value of Z. The difference between these two values can be caused by a different layer thickness δz but also, and more importantly, by a different mean fall speed. Indeed, smaller raindrops with lower fall speeds will not contribute to the mean fall speed of the total amount of water that crosses the bottom of the layer. The latter is consequently higher than the mean fall speed of all the water available in the layer.

A good guess for this alternative fall speed can be found as follows: P_{local} determines the fraction of the total water content which will pass the layer's bottom. When imaginary putting the water content of the layer at the top of this layer, then P_0 determines the fraction that will cross the layer's bottom. From these two expressions, one can compute the mean fall speed which the water at the top should have such that an equal amount of water will cross the layer's bottom than when the water was homogeneously distributed inside the layer. Mathematically this can be expressed as $P_0(Z^*) = P_1(Z)$ with $Z^* = \delta z^*/(\overline{w}^*\delta t)$ determined by the layer thickness δz^* and mean fall speed $\overline{w}^*$ of the layer above. P_{trans} inside a layer should then be computed using $Z' = \delta z/(\overline{w}^*\delta t)$ instead of Z.

One now has two solutions for the probability associated with precipitation coming from the layers above. Argumentation for which solution becomes our choice is given in Section 3.4.

3.3. *Expressions using a step function*

The final expressions of the probabilities associated with the different types of precipitation are constrained by the chosen expression for the PDF P_0. One can of course search for alternative expressions and an example is shortly developed below.

The basis is the following step function:

$$Q_0(Z) = \begin{cases} 1 & \text{if } Z \leq 1 \\ 0 & \text{if } Z > 1 \end{cases} \tag{11}$$

The three probabilities are then obtained as

$$Q_1(Z) = \min\left(1, \frac{1}{Z}\right) \tag{12}$$

$$Q_2'(Z) = \max(0, 1 - Z) \tag{13}$$

$$Q_3(Z) = \begin{cases} 1 - \frac{Z}{2} & \text{if } Z \leq 1 \\ \frac{1}{2Z} & \text{if } Z > 1 \end{cases} \tag{14}$$

One easily finds back

$$Q_3 = \frac{1}{2}(Q_2' + Q_1) \text{ and } Q_{\mathrm{trans\_sta}} = Q_2 = \frac{Q_2' + Q_3}{1 + Q_3}. \tag{15}$$

The step function scheme, using Q_{local}, Q_{trans} and $Q_{\mathrm{cre/des}}$ is constructed to reproduce advective sedimentation. This approach has been proposed at Météo-France to mimic the former operational Lagrangian scheme with a reduced numerical cost. As will be shown later in single column idealized tests, the results are very close to those of a purely advective sedimentation scheme. Q_0 is defined using the hypothesis that all the droplets have the same fall speed, and that is why it has the shape of a step function, all the droplets coming together out of the layer (or not). This hypothesis of a single fall speed is implicitly made in all numerical advective schemes for sedimentation. Q_{local}, Q_{trans} and $Q_{\mathrm{cre/des}}$ are then constructed by integration over space and/or time of the basic PDF Q_0 (same equations as (1), (2) and (3) of Section 3). To compute Q_{trans} by integration over the time step (like for P_{trans} in the other formulation) it is necessary to make the additional assumption that the incoming flux at the top is constant during the time step. This is the only thing that will make the results differ from the Lagrangian sedimentation scheme. The impact is a slight dispersion of the droplets along the vertical, linked to Z: the smaller Z, the bigger the dispersion. This can be interpreted as a kind of CFL criterion, but for accuracy rather than for stability. The PDF scheme using the step function has been implemented in the operational global model ARPEGE and also in the limited area model (LAM) ALADIN-France, in replacement of the original Lagrangian scheme. The results concerning the precipitation fields are quasi-identical.

From the lower panel of Fig. 1 (see the next subsection for more explanations about the figure), one sees that the associated set of probability profiles does not obey the constraint $Q_2 \geq Q_3$.

On the other hand, these probabilities are directly designed to mimic a well-defined pure advective sedimentation scheme, as explained above and as will be verified in Section 4. Hence there seems to exist some paradox, which we shall try to explain now.

Generally speaking, the absence of a correct stationary solution has to do with the limitation of the model's 'time step to time step memory' to the average properties of the prognostic falling species inside each layer. For the mass variable, this amounts to a systematic (and implicit) redistribution at each time step, which has nothing to do with the true sedimentation process. There are however two distinct causes for the need for redistribution. As already mentioned in Section 3.2, a too short time step will lead to an 'acceleration' of the apparent fall of the species, whatever method is used. In the present case of a unique fall speed, the redistribution process is also needed because the translation from each layer's content at the beginning of the time step only partly fills other layers (or itself) at the end of the time step. Even more, this happens in a repetitive way. Hence we get a kind of noise-generating effect that prevents the establishment of a stationary solution even at high Courant numbers. Of course, this second syndrome disappears when using a PDF that implies a spectrum of fall speeds, since the arrival locations are then implicitly more or less randomly distributed across the layers. The fact that the Q-type computations are nevertheless yielding reasonable results in transient mode (see below), even in the Q_{trans} version, probably indicates that the generated 'noise' is kept within acceptable limits, at unbiased average impacts for high enough Courant numbers.

It should also be noted here that, while the use of the step function does not fundamentally change the numerical behaviour of the proposed scheme, it leads to the loss of the property of self-preservation of the PDF shape along the fall-paths (linked to the specific choice of the decreasing exponential). As will be shown below, this does not seem to have any practical negative consequence. Nevertheless, in order to mark the difference in the conceptual choices, we shall from now on reserve the expression 'statistical scheme' exclusively for the decreasing exponential case and use the 'PDF-based scheme' expression for the wider method of applying three probabilities of 'escape', independently on the way they were analytically obtained. Hence the second denomination encompasses the first one, which initially triggered this enlarged study.

3.4. *Illustrations of the various expressions*

The different probabilities derived in this Section are plotted in Fig. 1. Apart from the initial three probability functions $[P_1(Z), P_2'(Z)$ and $P_3(Z)]$ and the basic PDF $P_0(Z)$, the top panel of Fig. 1 also shows $P_2(Z)$ and $P_2'(Z')$ (with Z' in the case of constant layer thickness throughout the vertical). It is clear that $P_2(Z)$ obeys the condition $P_2 \geq P_3$ far better than $P_2'(Z)$ and also better than $P_2'(Z')$. It therefore becomes our choice by default when trying to simulate the sedimentation properties of precipitations having non-uniform fall-speeds. The lower panel of Fig. 1 shows the alternative PDF Q_0 and the Q-probabilities associated with the step function.

3.5. *Drop-size distributions*

While an advective method will use the fall speed to determine the travelled distance of precipitation, the PDF-based method will use this fall speed to compute the fraction of the precipitation that will cross the bottom of the layer under consideration. Both methods use a single fall speed but the latter approach is probably a bit more realistic. A comparison between the drop-size distributions implicitly used by both methods and the Marshall–Palmer law of drop-size distribution (see Marshall and Palmer, 1948) should illustrate this. Below is a guide on how to find these drop-size distributions. Since some arbitrary assumptions are to be made (e.g. the fall speed dependency on the raindrop diameter, etc.), the final comparison will only be a qualitative one.

The distribution associated with the statistical scheme can be found by identifying the PDF $P_0(\delta z, \delta t)$ and the fraction of the total rain-water which will cross the layer. The latter can be expressed as the ratio of the integral of the rain-water flux [which implies the 'to be found' distribution $X(D)$] over a limited spectrum in raindrop diameters D (drops with a diameter smaller than a certain value D_0 will not cross the layer) and the integral over the full diameter spectrum. This writes:

$$\frac{\int_{D_0}^{\infty} D^{3+\alpha} X(D)\,\mathrm{d}D}{\int_{0}^{\infty} D^{3+\alpha} X(D)\,\mathrm{d}D} = \exp\left[-\frac{\delta z}{a\delta t}\frac{\int_0^{\infty} D^3 X(D)\,\mathrm{d}D}{\int_0^{\infty} D^{3+\alpha} X(D)\,\mathrm{d}D}\right], \quad (16)$$

where we assume that the diameter dependence of the fall speed can be expressed as $V = aD^{\alpha}$ (α and a can be determined from observations). Assuming that $X(D)$ takes an exponential form, or $X(D) = \exp(-\,bD)$, one can write

$$\frac{\int_{D_0}^{\infty} D^{3+\alpha} \exp(-bD)\,\mathrm{d}D}{\int_{0}^{\infty} D^{3+\alpha} \exp(-bD)\,\mathrm{d}D} = \exp\left[-\frac{\delta z}{a\delta t}\frac{\int_0^{\infty} D^3 \exp(-bD)\,\mathrm{d}D}{\int_0^{\infty} D^{3+\alpha} \exp(-bD)\,\mathrm{d}D}\right], \quad (17)$$

which can be rewritten as

$$\frac{\boldsymbol{\Gamma}(4+\alpha, bD_0)}{\Gamma(4+\alpha)} = \exp\left[-\frac{b^{\alpha}\,\delta z}{a\,\delta t}\frac{\Gamma(4)}{\Gamma(4+\alpha)}\right]. \quad (18)$$

Keeping α and a fixed, a given value for $\delta z/\delta t$ yields (a bit arbitrarily) a value for D_0. From the expression above one can then compute b. The final expression for $X(D)$ has of course some scaling factor so that $X(D) = X_0 \exp(-\,bD)$. X_0 can be found by integrating both the Marshall–Palmer distribution $[N(D) = N_0 \exp(-\lambda D)]$, with N_0 a scaling factor and λ a measure of the rainfall intensity) and the one associated with the statistical sedimentation over the full spectrum of rain drop sizes. Assuming that both integrals should have the same value, one can write

$$\int_0^\infty N(D)\frac{\pi D^3}{6}\,\mathrm{d}D = \int_0^\infty X(D)\frac{\pi D^3}{6}\,\mathrm{d}D. \tag{19}$$

This yields

$$X(D) = X_0\exp(-bD) = N_0\left(\frac{b}{\lambda}\right)^4\exp(-bD). \tag{20}$$

Because of the λ-dependency of X_0, different rain intensities will create different intersections of the X-distributions with $D = 0$.

The advective points, which are a Dirac-type distribution, follow from the identification of the total water mass in the Marshall–Palmer case and in the advective case. Assuming a constant fall speed and keeping α fixed, one can find a value for the single diameter D_a. The identification can be written as

$$N_{\mathrm{adv}}\frac{\pi D_a^3}{6} = \int_0^\infty N_0\exp(-\lambda D)\frac{\pi D^3}{6}\,\mathrm{d}D = N_0\frac{\Gamma(4)}{\lambda^4}\frac{\pi}{6}, \tag{21}$$

from which one can compute N_{adv}.

Figure 2 gives a qualitative comparison between the three types of raindrop size distribution (once again, the methods for drawing each part of the diagram differ too much for speaking of a quantitative comparison): (i) the classical (but close to observations) Marshall–Palmer distribution for three different rainfall rates (25 mm h^{-1}, 5 mm h^{-1} and 1 mm h^{-1}); (ii) the distributions associated with the statistical sedimentation scheme for the same rainfall rates and (iii) the Dirac-type distribution associated with a single fall speed of 5 m s^{-1} for the advective case (again for the three rainfall rates). The figure shows that the statistical approach corresponds to a raindrop size distribution which is nearer to observations than the Dirac-type distribution corresponding to an advective scheme, even if being by far less spectrally selective than the Marshall–Palmer one.

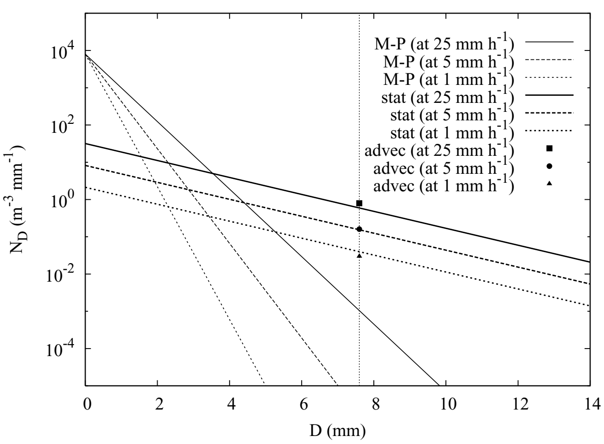

Fig. 2. A (qualitative) comparison between the Marshall–Palmer drop-size distributions *(M–P)* for three rainfall rates, the drop-size distributions associated with the statistical sedimentation scheme (stat) and the drop-size distributions associated with an advective sedimentation scheme (advec). Indications on how to reproduce these examples of distributions are given in the text.

4. Academic single column tests

4.1. Description and setup

The purpose of an academic test environment is twofold: (1) to have a tool in which the sedimentation process is isolated from all other microphysical processes and (2) to be able to compare the behaviour of the proposed PDF-based schemes with a reference scheme relying on the Marshall–Palmer distribution and with a pure advective scheme. Unfortunately, the envisaged isolation of the sedimentation process implies that the behaviour of $P_{\mathrm{cre/des}}$ or $Q_{\mathrm{cre/des}}$ cannot be tested in this environment. The 3-D tests reported in Section 5 however suggest (not shown) that these probabilities do what they are designed for.

The basic setup of the single column model is as follows.

(1) The model evidently allows only vertical movement of rain.

(2) The profiles for pressure and temperature are the ones of the standard atmosphere: $T_0 = 20\,^\circ$C, $p_0 = 1013.25$ hPa, temperature lapse rate: 6.5 $^\circ$C km^{-1} (up to 12 km).

(3) The length of the time step can be chosen as desired.

(4) The layers are equally spaced in height.

(5) Since the height of the vertical column is fixed, the number of layers (which can be chosen as desired) will determine the vertical resolution.

(6) The vertical resolution and the time step length together give a measure of the inverse Courant number Z.

(7) On the first time step rain-water is inserted between 6000 and 8000 m: each layer in this interval has a rain-water mass ratio $q_r = 0.0002$.

(8) At the beginning of each time step the rain-water is assumed to obey the Marshall–Palmer drop-size distribution at all heights.

The model has a choice between two types of schemes.

(i) The PDF-based ones, based on the different expressions for the probabilities. They can use either a variable fall speed (depending on the rain intensity) or a fixed fall speed. Concerning the choice of the P/Q_{local} and P/Q_{trans} (or $P\,/\,Q_{\mathrm{trans\_sta}}$) functions, no hybrid combination is allowed, even in the cases reported in Section 4.5.

(ii) The reference one. It can use either a spectrum of fall speeds (according to the observed fall speed dependency on the raindrop diameter) or a single fixed fall speed (like a typical advective scheme).

A short description of the followed strategy for these two types of schemes is given below.

The first step in the PDF-based schemes is the computation of the average fall speed (at least if it is not taken to be a constant of 5 m s^{-1}) of the rain-water inside a layer. A derivation similar to the one in Liu and Orville (1969) gives the following expression:

$$\overline{w} = 1857.7 \left(\frac{\rho_0}{\lambda \rho} \right)^{0.77}, \tag{22}$$

with ρ the air density, ρ_0 the air density at the surface and λ the rain intensity parameter of the Marshall–Palmer law. Next, the scheme computes the probabilities P_{local} and $P_{\mathrm{trans\_sta}}/(P_{\mathrm{trans}})$ [or Q_{local} and $Q_{\mathrm{trans}}/(Q_{\mathrm{trans\_sta}})$ as an alternative] which will then determine the fraction of the total water content that will cross the bottom of the layer. Finally, after the transport of the rain-water, each model layer is forced to obey the Marshall–Palmer distribution again.

Instead of using a mean fall speed, the reference schemes will divide the range of drop sizes (between 0 and 1 cm) in 100 intervals and for each interval a fall speed is computed (with a spectrum of fall speeds as result). For this a relation between the diameter D of a raindrop and the associated fall speed is derived (again similar to Liu and Orville, 1969):

$$w = 654.5 \left(\frac{\rho_0 D}{\rho} \right)^{0.77}. \tag{23}$$

Drops with diameters bigger than 1 cm are assumed to have an infinite vertical velocity. For each drop-size interval the scheme computes the associated mass of rain-water and from both the mass and fall speed it computes the total rain-water flux through the bottom of each layer. Finally, as in the PDF-based schemes, at the end of the time step each model layer is forced to obey the Marshall–Palmer distribution.

The reference scheme with a single constant fall speed is similar to the one above except that the same fall speed of 5 m s^{-1} is associated with each drop-size interval.

Both reference schemes (with either a variable or constant fall speed) are Lagrangian advective schemes (with a double loop to determine how far the rain-water falls and using a box-type method for redistribution). Comparison of the two nearly overlapping curves in the upper panel of Fig. 4 (more about this figure in Section 4.3) seems to indicate that this advection method is hardly affected by numerical diffusion. The PDF-based schemes on the other hand obviously cannot be categorized as advective schemes. The tendency of the rainwater mass ratio in a layer is computed in all schemes as the (discrete) divergence of the precipitation flux.

None of the schemes described above keeps track of the number of drops during the sedimentation process, a property which makes them all equivalent to single-moment schemes. The performance of PDF-based sedimentation in something equivalent to a double-moment scheme is given in Section 4.5.

Equations (1) and (2) [or (10)] show that P_{local} and $P_{\mathrm{trans\_sta}}$ depend entirely on Z. Although the freedom in the academic framework allows a wide range of Z, tests will be restricted to three characteristic values: $Z \sim 0.2, 2$ and 20 (by using a vertical resolution of respectively, 1, 10 and 100 m and a 1 s time step). Those three Z-values were chosen for the following reasons. The bigger one corresponds to cases where one does not expect any divergence between various methods, something still to be verified for the algorithm proposed here. The medium one corresponds to the practical CFL condition limit (0.5 rather than the theoretical 1.0 value) for advective sedimentation schemes. The smaller one corresponds to the type of Courant number which one may encounter in the lower levels of an ALADIN run at kilometric horizontal mesh-size (time step of the order of 40 s) with about 50 vertical levels (lower model level 40 m thick) and with an average fall speed for rain of 5 m s^{-1}.

A distinction will also be made between cases where a spectrum of fall speeds is used and cases where a single constant fall speed is used. The former is considered to be closer to reality while the latter corresponds to the idea behind most advective sedimentation schemes used nowadays inside numerical models.

4.2. Experiments using a spectrum of fall speeds

As already mentioned in Section 3, the initial tests did not give very satisfying results for P_{trans}, in particular for low values of Z. This is illustrated in the upper panel of Fig. 3 which is valid for $Z \sim 0.2$. In this panel the surface precipitation flux is plotted as a function of time for 5 cases: the reference scheme and the PDF-based scheme using either $P_2'(Z), P_2(Z), P_2'(Z')$ or $Q_2(Z)$. The centre and lower panel show similar curves but for $Z \sim 2$ and $Z \sim 20$, respectively.

From the upper panel it is immediately clear that for this value of Z a scheme which uses $Q_{\mathrm{trans\_sta}}$ is not able to simulate the sedimentation process in a satisfying way (i.e. the corresponding curve is far from the reference one, in terms of both timing and maximum intensity, with the Dirac-like shape peaking at about 200 g m^{-2} s^{-1}). This is not surprising since for $Z < 1$ $Q_1 = 1$ and Q_2 is close to 1, which results in a very fast sedimentation process. Remember also that the Q-probabilities were designed to mimic an advective sedimentation process with a constant fall speed which is quite different from one with a variable fall speed. The bad results of the initial probability P_{trans} are significantly reduced by using either $P_{\mathrm{trans\_sta}}$ or $P_2'(Z')$. Even if the results are then far from perfect, one should not forget that gaining a substantial factor in numerical efficiency and/or streamlining a basically complex code allows to dedicate more efforts to the accurate description of the creation and disappearance processes for the falling species. As already said, the simulation of those complex processes is out of the scope of the idealized experiments reported in this Section. But one knows that their influence on the complete precipitation processes is stronger than the one of sedimentation. This will be indirectly verified in the full 3-D example reported in Section 5 where, with a horizontal mesh size of 9 km, Courant numbers even up to 50 will be used near the surface, without any apparent degradation of the forecast surface precipitation fields' quality.

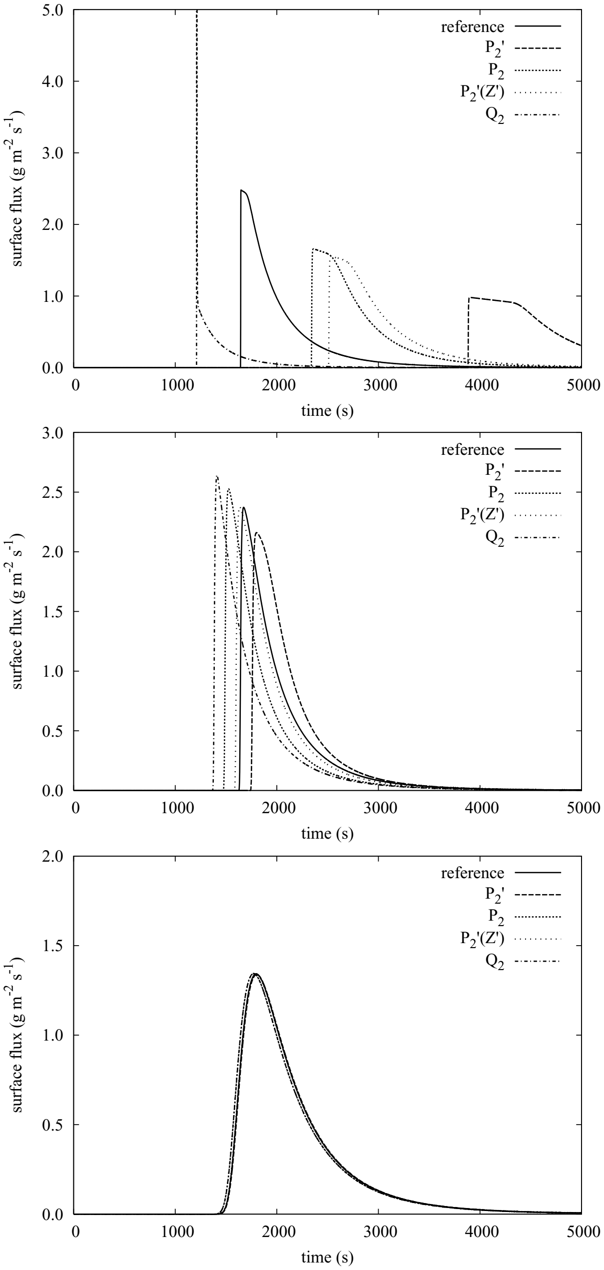

Fig. 3. The surface precipitation flux as a function of time for five cases with a variable fall speed (see text). The value of Z (inverse of the Courant number) is different for each panel and is around 0.2, 2 and 20 for, respectively, the upper, centre and lower panel. Note that in the lower panel the curves of the reference, P_{trans} and $P_2'(Z')$ cases are superimposed as well as the curves of the P_2 and Q_2 cases.

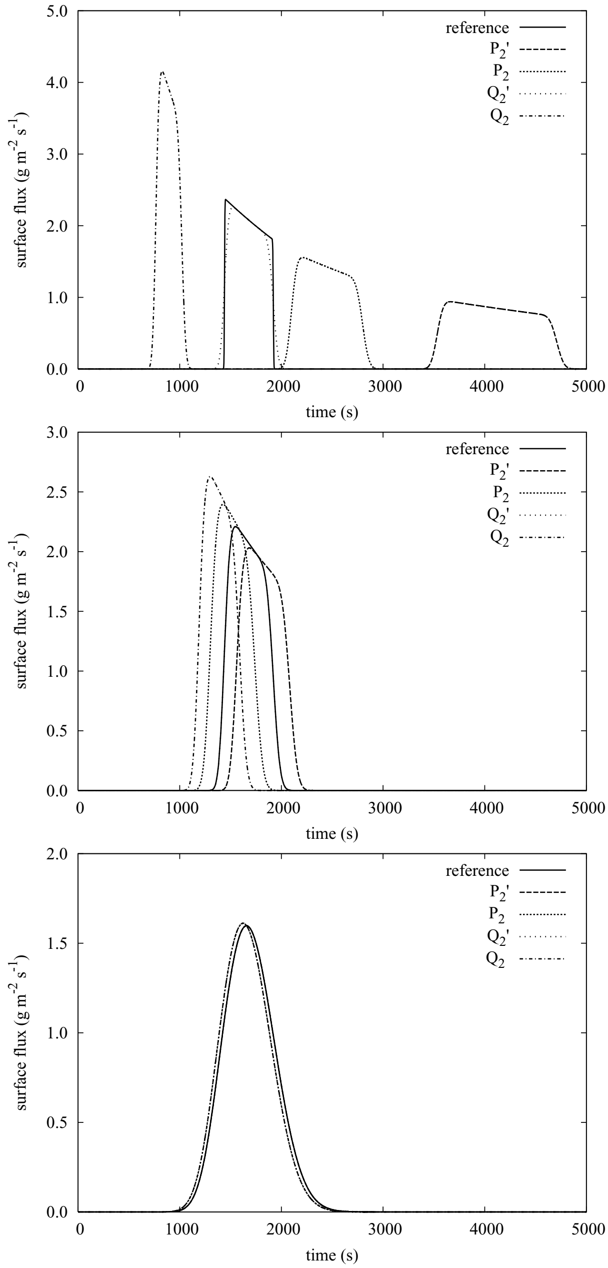

Fig. 4. The surface precipitation flux as a function of time for five cases with a constant fall speed (see again text). The value of Z (inverse of the Courant number) is different for each panel and is around 0.2, 2 and 20 for, respectively, the upper, centre and lower panel. Note that in the lower panel the curves of the reference, P_2' and Q_2' cases are superimposed as well as the curves of the P_2 and Q_2 cases. In the middle panel, the curves of the reference and of the Q_2' case are also superimposed.

When increasing Z (centre and lower panel) all PDF-based cases move gradually towards the reference case. The slightly slower fall corresponding to $P_2'(Z')$ (when compared to $P_{\mathrm{trans\_sta}}$) is sometimes a handicap and sometimes an advantage during this convergence.

4.3. Experiments using a single constant fall speed

In Fig. 4 similar curves as in Fig. 3 are drawn but now a fixed fall speed of 5 m s^{-1} is used in all schemes. In the upper panel the surface precipitation flux is plotted as a function of time for the following 5 cases (still at $Z \sim 0.2$): the reference scheme and the PDF-based scheme using either P_2', P_2, Q_2' or Q_2. The centre and lower panel show similar curves but for $Z \sim 2$ and $Z \sim 20$, respectively. Immediately, one notices the almost perfect behaviour of the Q_{trans} case for all values of Z (the small deviations at the edges of the shape in the upper panel are in fact due to the redistribution after each time step). $Q_{\mathrm{trans\_sta}}$ on the other hand gives poor results. This difference with the results shown in Fig. 3 can be attributed to the fact that the definition of Q_{trans} is based on a homogeneous arrival in time of raindrops at the top of a layer. This is of course valid when using a constant fall speed and therefore an extension towards $Q_{\mathrm{trans\_sta}}$ is not needed here. For P_{trans}, which was initially designed for sedimentation with a spectrum of fall speeds, and contrary to the 'Q-case', the change towards $P_{\mathrm{trans\_sta}}$ is still necessary for getting better results at low values of Z.

Comparison of the reference cases in Figs. 3 and 4 also illustrates the big difference of the to be simulated sedimentation process when using either a spectrum of fall speeds or a single constant fall speed.

4.4. Discussion

The two subsections above suggest that PDF-based sedimentation schemes are able to qualitatively simulate the sedimentation process inside a microphysical scheme. What is more, from four possible sets of probabilities, only two make sense. Indeed, the sedimentation process when using a spectrum of fall speeds can be mimicked rather well with the $P_{\mathrm{trans\_sta}}$ solution. In the case of a constant fall speed Q_{trans} is the best solution.

An additional illustration of the performance of the statistical approach is given in Fig. 5 where 'cloud shapes' for different cases are plotted when $Z \sim 2$. These cloud shapes are in fact the amount of water (represented by q_r) inside the vertical column still present after 20 minutes. In order not to overload the figure, we only consider the following cases: the reference case, the $P_{\mathrm{trans\_sta}}$ case and the $P_2'(Z')$ case (all using a spectrum of fall speeds) and the reference case when using a single constant fall speed (the constant being the mass averaged fall speed). The statistical cases are very similar to the curve of the reference case (when using a spectrum of fall speeds) which confirms the ability of the statistical approach to treat dispersive sedimentation in a close to reality way, despite the differences in spectral slope illustrated by Fig. 2. The reference case with a constant fall speed was added to the figure to illustrate once again the difference in the to be simulated process between the close to reality dispersive curves (associated to a spectrum of fall speeds) and the bulk-transport curve associated with a typical advective sedimentation scheme (associated to a unique constant fall speed). Adding the Q_{trans} result to the diagram would not have brought any additional information, so close is its result with its non-dispersive target.

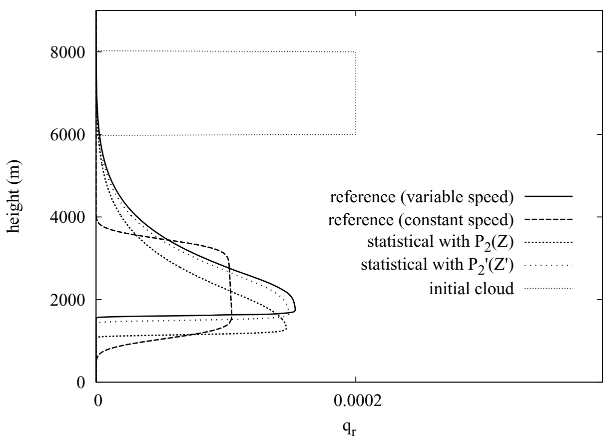

Fig. 5. Cloud shapes, that is, the amount of water inside the vertical column still present after 20 min, for the different schemes using $Z \sim 2$. The initial cloud shape is also presented.

4.5. Double-moment sedimentation schemes

As already mentioned, the different sedimentation schemes described in the subsections above are so-called single-moment schemes. Indeed, only the rainwater content is considered as a prognostic quantity and after each time step a renormalization of the raindrop distribution occurs (explicitly in the academic tool for the reference computations and implicitly in the proposed versions of the statistical method). Double-moment sedimentation schemes which describe the sedimentation of precipitation by two prognostic quantities have proven to better reproduce the processes leading in nature to the equivalent of this renormalization, see for example, Wacker and Seifert (2001), WS01 hereafter. But they also encounter additional numerical hurdles when the sedimentation process is considered in isolation, alike in the single column tests reported just above (see again WS01). Now that we demonstrated the performance of PDF-based sedimentation in a single-moment single column framework, we may turn our attention towards double-moment schemes.

Of course, the PDF-based sedimentation computation itself cannot be catalogued as a single or more moment scheme. It only tries to replace the advective character of existing sedimentation schemes (which require either a double vertical loop or a specific fractional time stepping) by a probability approach (which can be done in a single space–time computational loop). This subsection will explore what happens when replacing the advective steps inside a double-moment sedimentation scheme with elements of a PDF-based approach, without reconsidering here the latter's basic characteristics.

For this, the single column model previously described is extended with a second moment of sedimentation, that is, the number of raindrops present in a model layer. A second change in the test tool is that there is no longer a redistribution towards the Marshall–Palmer drop-size distribution at the end of each time step. With these two changes, the single column model is able to simulate or mimic a double-moment scheme. The previous (single-moment) reference scheme is now becoming a kind of double-moment bin model and will be called henceforth the double-moment reference scheme.

A first type of experiment is performed by replacing the advective approach in this new reference scheme by the PDF approach. Since the PDFs based on the step function (eqs. 12–13) are very good in reproducing advective-type sedimentation, they will be used in this experiment.

A second type of experiment is performed by replacing the advective approach in an existing double-moment parametrization by the PDF approach. The double-moment scheme which will be used is the one described in Section 4 of WS01. Here also, the probability functions directly based on the step function will be used. What is more, WS01 reported a 'shock-wave' effect when using their parametrization. In order to check this effect with our PDF approach, the experimental setup was made as close as possible to the setup described in their Section 4. This means a vertical grid spacing of 30 m and a minimal number of drops $N_{\min} = 10^{-12}$ cm^{-3}.

The resulting cloud profiles after 300 s for these two types of experiments are shown in Fig. 6. More precisely, the following cases are shown: the double-moment reference scheme when using advective sedimentation; the double-moment-type reference scheme when using PDF-based sedimentation with Q_{trans} (bin model like experiment); the WS01 scheme when using advective sedimentation; the WS01 scheme when using PDF-based sedimentation with Q_{trans}; and finally the WS01 scheme when using

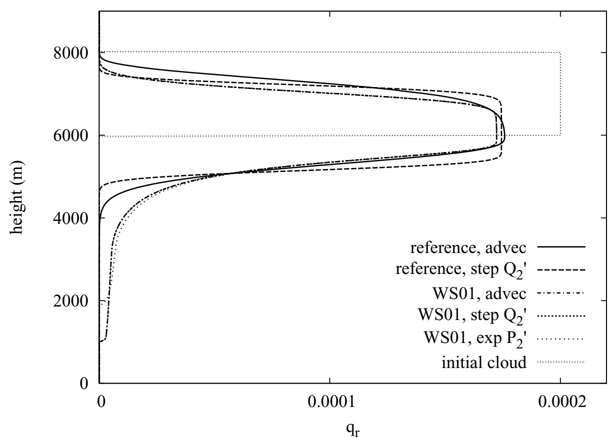

Fig. 6. Cloud shapes, or the amount of water inside the vertical column, after 300 s for the following cases: the double-moment reference scheme with advective and PDF-based sedimentation, the WS01 double-moment scheme with advective sedimentation and the WS01 double-moment scheme with PDF-based sedimentation when using either Q_2' or P_2'. Note that the curves for the WS01 double-moment scheme with advective sedimentation and with PDF-based sedimentation when using Q_2' are superimposed. The initial cloud profile is also shown.

PDF-based sedimentation with P_{trans}. This figure proves that the PDF-based sedimentation with Q_{trans} is able to exactly mimic advective-type sedimentation in double-moment schemes. Note indeed that the curves for the WS01 double-moment scheme with advective sedimentation and with PDF-based sedimentation when using Q_{trans} are superimposed. This of course illustrates the not too surprising fact that the use of the PDF-based method also produces the shock-wave, inherent to the setup of the WS01 parametrization. However, when using the probability functions directly based on the decreasing exponential instead of the ones based on the step function we are able to reduce the shock-wave a bit, but certainly not sufficiently to claim proposing a new solution when simply extrapolating our single-moment oriented first solutions towards this new problematic.

Coming back now to Section 3, we may present its two main findings (and their separate mathematical and physical justifications) in the following way. While searching to replace advective-type sedimentation computations by something simpler and cheaper at equal or better accuracy, we heuristically discovered two degrees of freedom potentially leading to a family of schemes. The first one is the choice of the basic PDF (P_0/Q_0 in the reported examples) while the second one is the way to choose the 'transmission' probability through the layer, once the basic PDF is known. In the present study, we considered only a 2×2 matrix among a far bigger set of possibilities and only two of the four combinations made sense (with opposite choices for each degree of freedom). It is likely, but this surely goes beyond the scope of what we wish to report here, that other yet unexplored combinations would also make sense and maybe even more sense than what was studied here in detail. And it might well be, given the last result of the previous paragraph, that the search for a solution fully avoiding the shock-wave syndrome in the equivalent to a double-moment advective scheme would become an excellent guideline for the search of such better results. Of course, one cannot be too affirmative about the chances of success of such a further study.

5. 3-D ALARO-0 tests

In the previous Section a number of academic-type experiments showed the accuracy and flexibility of the PDF-based method for sedimentation of precipitation. In this Section the performance of such a sedimentation scheme will be demonstrated in a complete NWP context. The basic application will be the ALADIN forecasting system at the Czech Hydrometeorological Institute (CHMI), based on an intermediate version of the ALARO-0 physical package, operational at CHMI since the end of January 2007. The horizontal mesh-size is 9 km, the time step 360 s and the number of vertical levels 43. The diagrams will only display a small part of the model integration domain, a zoom effect being here the best way to compare various setups for the sedimentation process (the larger scale patterns are hardly affected by the choice of tested options).

ALARO-0 has an acronym resulting from the contraction of the ALADIN and Application de la Recherche à l'Opérationnel à Moyenne Echelle (AROME) ones with the adjunction of the base-line-version-characterizing zero. This package attempts at combining ascending compatibility with previous more classical ALADIN versions, orientation towards a maximum of prognostic variables, modularity- and multiscale character as well as numerical- and algorithmic efficiency. The level of complexity of the basic parametrized physical processes is chosen as intermediate, in accordance with a primary aim of the said package at horizontal mesh-sizes of about 5 km.

The cloud and precipitation microphysical scheme reflects all these characteristics. The sedimentation is of course treated in the cost-efficient and structuring PDF-based way. The evaporation and melting-freezing of falling rain and snow use similar setups as for the previous diagnostic-only ALADIN scheme (Geleyn et al., 1994). The collection part is identical to that of Lopez (2002) but for a differing dependency upon density and with slightly simplified temperature dependencies. The autoconversion part also uses temperature dependencies simplified from those of Lopez (2002), its basic formulation is the one of Sundquist (1978) and it is extended to encompass the Wegener–Bergeron–Findeisen process in a manner similar to Gerard (2007) on the basis of van der Hage's (1995) interpretation.

One shall deal here primarily with the sedimentation part of this new microphysical scheme, since details of the other features do not matter for the demonstration at the heart of the present paper. The test case is that of a large-scale precipitating area which crossed Central Europe on the 5th of November 2006 and which produced locally some intense rainfall (especially over mountain ridges). The domain of display is centred over the Czech Republic and the tests are performed using the now operational CHMI framework on this interesting pre-operational (at the time) situation.

Figure 7 shows the 6 h accumulated surface precipitation after 18 h of integration for four different setups of the sedimentation process:

(i) *Reference scheme:* uses the P-type PDF-based sedimentation, with variable fall speed. This corresponds in fact to the 'statistical' sedimentation using the $P_{\mathrm{trans\_sta}}$ function.

(ii) *Lagrangian-like scheme:* uses the Q-type PDF-based sedimentation, with fixed fall speeds of 4.5 and 0.9 m s^{-1} for, respectively, rain and snow. This corresponds to the 'advective' sedimentation (remember the good resemblance between advective sedimentation and the Q_{trans} function sedimentation).

(iii) *High speed scheme:* the setup is like in 'reference' but one uses quasi-infinite fall speeds. This mimics the removal of precipitation within a single time step.

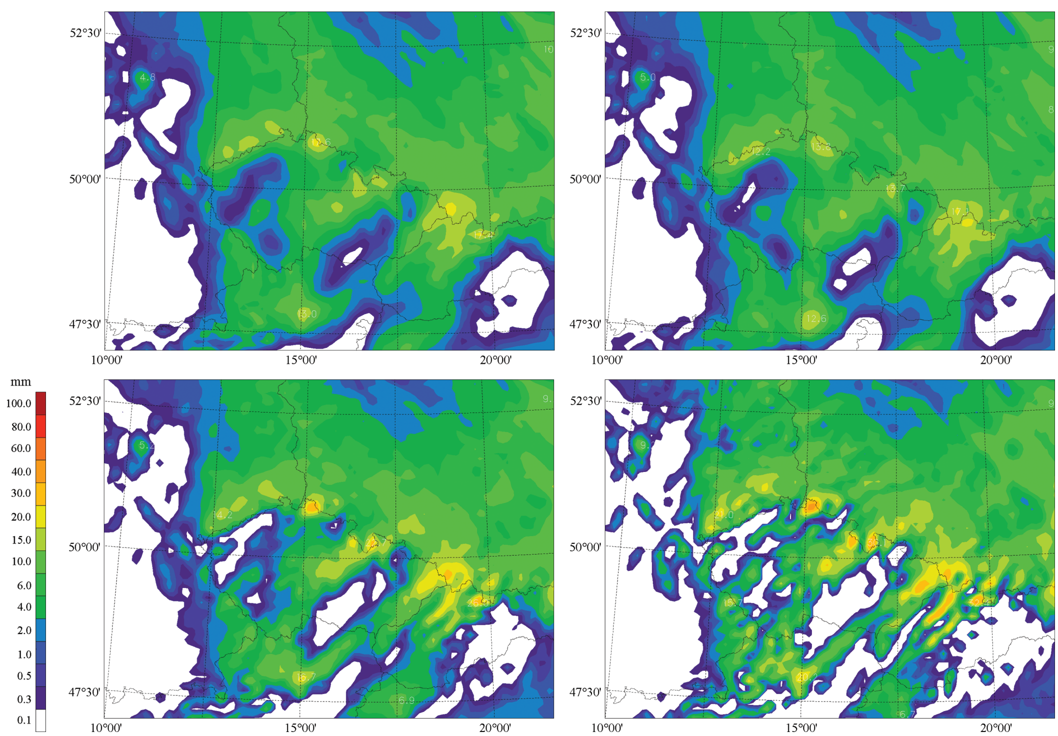

Fig. 7. ALADIN-CE 18 h forecasts starting from 5 November 2006 00UTC: 6 h cumulated surface precipitation amounts (in mm) over the territory of the Czech Republic for four different setups of the sedimentation process (top left-hand side = reference scheme; top right-hand side = Lagrangian-like scheme; bottom left-hand side = high speed scheme and bottom right-hand side = old scheme).

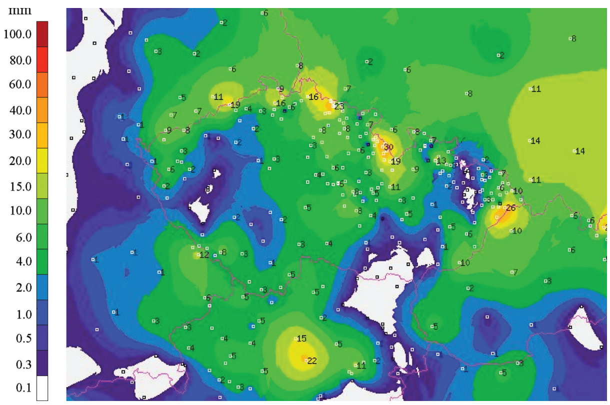

Fig. 8. Observed surface precipitation amounts from rain gauge data for a similar area and for the same 6 h period as in Fig. 7 (5 November 2006 12UTC–5 November 2006 18UTC). The colour scale (for precipitation rates in mm per 6 h) is identical to the one of Fig. 7. For the positioning with respect to the latter, the upper left-hand corner of Fig. 8 is at 10°07′E–51°43′N and its lower right-hand corner at 20°05′E–47°13′N.

(iv) *Old scheme:* uses the former diagnostic precipitation scheme. Besides the sedimentation process the prognostic microphysical scheme also upgraded other parts (only the autoconversion one having here a marked impact, of course), which explains the somewhat differing results from those of the 'high speed' case.

For an objective comparison, the observed precipitation from rain gauge data is shown in Fig. 8. Comparison of the four simulations reveals two groups of two experiments: the reference scheme together with the Lagrangian-like one (top row of the figure) and the high speed scheme together with the old one (bottom row of the figure). The first group proves the stability of the proposed PDF-based sedimentation scheme: whether one uses the P-type probabilities or the Q-type ones (or very likely any other set of well designed probabilities), the sedimentation process and consequently the resulting precipitation distribution are very similar. Furthermore this common result is far more realistic than the 'old' one, since for instance the precipitation maxima are displaced towards the mountain ridges and do not stay erroneously on the windward slopes. The general shape of the precipitation pattern is also far better for the top row results than for the bottom row ones, when compared to observations. The progress in positioning the maxima over the ridges is more apparent with the 'Lagrangian-like' choice, but this result must be taken with caution since it may depend on the choice of the fixed fall speeds, which were taken in the reported test as the averaged ones of what the 'reference' scheme would have computed.

The second group of experiments displays the link between the PDF-based sedimentation (used this time with quasi infinite fall speeds) and the diagnostic scheme where precipitation was transported to the surface in a single time step. Both results indeed show the same (bad) localization of the precipitation maxima. More interestingly, comparing all four results, one sees that the former spurious scattered distribution of surface precipitation disappears in two steps: with the introduction of cloud water latency (between both results of the second group) and with the full introduction of the PDF-based sedimentation variants, alike it would be of course for any scheme having falling condensates as prognostic variables. As hinted at in the previous paragraph, the precipitation fields of the first group are indeed realistically much smoother than the ones of the second group, especially when considering the very scattered patterns of the 'old' scheme.

6. Conclusions

A PDF-based method for sedimentation of prognostic precipitating species inside a microphysical scheme of intermediate complexity (i.e. fully prognostic but without spectral decomposition of hydrometeor sizes) was developed and tested. Provided the other cloud and precipitation processes (autoconversion, collection, evaporation and melting-freezing of falling species, etc.) can be treated locally, as should in principle always be the case at the said intermediate level of complexity, it can be applied to any cloud and precipitation scheme. The basic formulation is simple (it relies on three analytical formulations for probabilities of 'escape' of all falling species from a given model layer) and its application is straightforward. Indeed, unlike for advective-type sedimentation methods, there is no more need for iterations in space or in time. The proposed scheme is thus absolutely stable and rather cost-effective.

The performance of this new method was demonstrated by experiments in both an academic and a full 3-D environment. The present study mainly focused on the performance with respect to single-moment schemes which are indeed the least complex environments for comparison, since they describe only one sedimentation process. Double-moment schemes on the other hand describe two different sedimentation processes at the same time (mass and number concentration) which makes the test-environment more complex. Nonetheless, it was shown that the PDF-approach, when compared with double-moment schemes, gives results that are neither degraded nor clearly enhanced with respect to the ones obtained in the basic single-moment framework.

It can be concluded from these experiments that the PDF-based approach is very flexible and delivers as realistic results as the advective methods it aims to replace. Indeed, different sets of probabilities are possible and give similar results. It was also shown that what was named P-type probabilities can mimic a sedimentation process with a full spectrum of fall speeds quite well. Furthermore, what was named Q-type probabilities can reproduce a sedimentation process with a fixed fall speed nearly perfectly. However, both results are obtained with different options for the way to determine the probability of 'transparent' transfer of falling species through any given model layer. The choice is then between a somewhat more realistic scheme that simulates the observed dispersive properties of sedimentation and the accurate and cheaper simulation of any well-tuned existing advective scheme. Of course other basic PDFs and/or ways to determine the best associated 'X_2' function could be proposed and might even combine the advantages of the two solutions described here, but this goes beyond the scope of this study.

Some upward compatibility with diagnostic-type schemes is also present in the proposal. When arbitrarily using infinite fall speeds, the PDF-based sedimentation scheme resembles the case where precipitation is transported towards the surface in a single time step without any prognostic treatment of the microphysical falling species. This property could be useful for validating the direct transformation of a diagnostic to a prognostic microphysical scheme, the latter being directly written in the formalism proposed here.

Finally, the PDF-based sedimentation scheme can be used in full 3-D NWP operational applications. Indeed this formulation has been in operational use (yet for stratiform precipitations only) at CHMI since 30 January 2007, with the basic 'statistical' $P_{\mathrm{trans\_sta}}$ choice. Later on, as already indicated, Météo-France similarly went to the 'Lagrangian-like' Q_{trans} choice for its versions of global and LAM applications.

7. Acknowledgments

We wish to thank M. Janoušek for his contribution to a more correct nomenclature. We are grateful to Météo-France and the Regional Cooperation for Limited Area modeling in Central Europe (RC LACE) programme for their financial support. All people contributing to the ALARO-0 R&D effort also created favourable conditions for this study and we wish to express here our gratitude to them. We also wish to thank the anonymous referees for their valuable suggestions which allowed us to present our findings in a more objective framework.

References

Catry, B., Geleyn, J.-F., Tudor, M., Bénard, P. and Trojáková, A. 2007. Flux-conservative thermodynamic equations in a mass-weighted framework. *Tellus* **59A**, 71–79.

Dare, R. A. 2004. The BMRC Bulk Explicit Microphysics (BEM) scheme. *BMRC Research Report, Melbourne, Australia* **99**, 110 pp.

Geleyn, J.-F., Bazile, E., Bougeault, P., Déqué, M., Ivanovici, V. and co-authors. 1994. Atmospheric parametrisation schemes in Météo-France's ARPEGE NWP model. In *ECMWF Seminar Proceedings on "Physical parameterisations in numerical models", 5–9 Sept. 1994*, ECMWF, Reading, UK, pp. 385–402.

Gerard, L., 2007. An integrated package for subgrid convection, clouds and precipitation compatible with meso-gamma scales. *Q. J. R. Meteorol. Soc.* **133**, 711–730.

Liu, J. Y. and Orville, H. D. 1969. Numerical modeling of precipitation and cloud shadow effects on mountain-induced cumuli. *J. Atmos. Sci.* **26**, 1283–1298.

Lopez, P. 2002. Implementation and validation of a new prognostic large-scale cloud and precipitation scheme for climate and data-assimilation purposes. *Q. J. R. Meteorol. Soc.* **128**, 229–257.

Marshall, J. S. and Palmer, W. McK. 1948. The distribution of raindrops with size. *J. Meteorol.* **5**, 165–166.

Reisner, J., Rasmussen, R. M. and Bruintjes, R. 1998. Explicit forecasting of supercooled liquid water in winter storms using the MM5 model. *Q. J. R. Meteorol. Soc.* **124**, 1071–1107.

Schultz, P. 1995. An explicit cloud physics parameterization for operational numerical weather prediction. *Mon. Wea. Rev.* **123**, 3331–3343.

Seifert, A. and Beheng, K. D. 2006. A two-moment cloud microphysics parameterization for mixed-phase clouds. Part I: model description. *Meteorol. Atmos. Phys.* **92**, 45–66.

Sundquist, H. 1978. A parameterization scheme for non-convective condensation including prediction of cloud water amount. *Q. J. R. Meteorol. Soc.* **104**, 677–690.

Van der Hage, J. C. H. 1995. A parameterisation of the Wegener-Bergeron-Findeisen effect. *Atmos. Res.* **39**, 201–214.

Wacker, U. and Seifert, A. 2001. Evolution of rain water profiles resulting from pure sedimentation: spectral vs. parameterized description. *Atmos. Res.* **58**, 19–39.

Wilson, D. R. and Ballard, S. P. 1999. A microphysically based precipitation scheme for the UK Meteorological Office Unified Model. *Q. J. R. Meteorol. Soc.* **125**, 1607–1636.